# The restricted active space followed by second-order perturbation theory method: Theory and application to the study of $CuO_2$ and $Cu_2O_2$ systems

Per Åke Malmqvist,[1] Kristine Pierloot,[2] Abdul Rehaman Moughal Shahi,[3] Christopher J. Cramer,[4] and Laura Gagliardi[3,a)]

[1]*Department of Theoretical Chemistry, University of Lund, P.O. Box 124, S-221 00 Lund, Sweden*
[2]*Department of Chemistry, University of Leuven, Celestijnenlaan 200 F, bus 2404,*
*B-3001 Leuven, Belgium*
[3]*Department of Physical Chemistry, University of Geneva, 30 Quai Ernest Ansermet,*
*CH-1211 Geneva, Switzerland*
[4]*Department of Chemistry and Supercomputing Institute, University of Minnesota, 207 Pleasant St. SE,*
*Minneapolis, Minnesota 55455-0431, USA*

A multireference second-order perturbation theory using a restricted active space self-consistent field wave function as reference (RASPT2/RASSCF) is described. This model is particularly effective for cases where a chemical system requires a balanced orbital active space that is too large to be addressed by the complete active space self-consistent field model with or without second-order perturbation theory (CASPT2 or CASSCF, respectively). Rather than permitting all possible electronic configurations of the electrons in the active space to appear in the reference wave function, certain orbitals are sequestered into two subspaces that permit a maximum number of occupations or holes, respectively, in any given configuration, thereby reducing the total number of possible configurations. Subsequent second-order perturbation theory captures additional dynamical correlation effects. Applications of the theory to the electronic structure of complexes involved in the activation of molecular oxygen by mono- and binuclear copper complexes are presented. In the mononuclear case, RASPT2 and CASPT2 provide very similar results. In the binuclear cases, however, only RASPT2 proves quantitatively useful, owing to the very large size of the necessary active space. © *2008 American Institute of Physics.* [DOI: 10.1063/1.2920188]

## I. INTRODUCTION

Accurate treatment of electron correlation is of paramount importance when *ab initio* quantum mechanical methods are applied to realistic chemical problems. Many chemical systems, especially those containing transition metals and heavier elements, cannot be well described using methods that depend on a single-determinantal Hartree–Fock (HF) reference wave function [a problem which can also diminish the utility of the Kohn–Sham formulation of density functional theory (DFT)]. Instead, a multideterminantal approach is needed, where the wave function is described as a combination of different electronic configurations. One of the most successful multideterminantal approaches is to determine a reference wave function with the complete active space self-consistent field (CASSCF) method and then account for additional electron correlation effects using a multiconfigurational second-order perturbation theory, e.g., CASPT2. The CASSCF/CASPT2 method has been demonstrated to provide accurate results for ground and electronically excited states of molecules containing atoms throughout the entire Periodic Table.[1–7] While in principle it can be applied to every type of electronic problem, there is a practical limitation associated with the size of the active space employed in the CASSCF model (see Sec. II).

We here describe an extension of the CASSCF/CASPT2 method, namely, the restricted active space (RAS)SCF/RASPT2 method. The RASSCF/RASPT2 model permits larger active spaces to be employed for the reference wave function and thus extends the range of multiconfigurational wave function methods to a wider variety of chemical problems. We note that Celani *et al.*[8] have previously described a model (CIPT2) having a similar motivation in which excitations solely from the active space are treated by multireference configuration interaction (MRCI) while all other excitations are treated by a second-order multireference perturbation theory. We anticipate that both models will serve as useful foundations for future development. Other MR perturbation theory models have been developed by Dyall,[9] Schmidt *et al.*,[10] Witek *et al.*,[11] and Angeli *et al.*[12]

The remainder of the paper is organized as follows: In Sec. II, the new methodology is described. In Sec. III, we present applications of the new model to supported $CuO_2$ and $Cu_2O_2$ systems, where it is challenging or impossible to apply conventional CASSCF/CASPT2. Some final discussion of possible future improvements in the theory is provided in Sec. IV.

---

a)Electronic mail: laura.gagliardi@unige.ch.

| | |
|---|---|
| **EXTERNAL** | All orbital have occupation number 0 |
| **RAS3** | Orbitals may have an occupation number from 0 to 2, but the maximum number of electrons in the space is limited to $n$ |
| **RAS2** | Orbitals may have an occupation number from 0 to 2 |
| **RAS1** | Orbitals may have an occupation number from 0 to 2, but the maximum number of holes in the space is limited to $n$ |
| **INACTIVE** | All orbital have occupation number 2 |

FIG. 1. A schematic representation of the orbital classification in the RASSCF method.

## II. METHOD

### A. The CASSCF/CASPT2 model

The CASSCF/CASPT2 model has been previously described in detail (Refs. 13 and 14, and references therein). We shall review here only those aspects of the method most relevant to its extension to the RAS implementation.

In a CASSCF wave function, the initial molecular orbital space (which may be taken from a HF calculation, for example) is divided into three subspaces: inactive, active, and external (see Fig. 1 with neither RAS1 nor RAS3 containing any orbitals). The inactive orbitals are assumed to be doubly occupied in all configuration state functions (CSFs) that are used to build the multiconfigurational wave function. The external orbitals are assumed to be unoccupied in all such CSFs. The remaining active orbitals include both occupied and virtual orbitals from the original molecular orbital space, and the number of electrons included in the active space is dictated by the number present in the occupied orbitals that are assigned to it. All CSFs having a given spatial and spin symmetry that can be formed from assignment of the active electrons to orbitals within the active space are included in the multiconfigurational wave function. The inactive orbitals then constitute a HF "sea" in which the active orbitals and CSF expansion coefficients variationally relax. This is the concept of the CAS introduced by Roos in the 1980s.[15,16]

Choosing the "correct" active space for a specific application is by no means trivial; often the practitioner must "experiment" with different choices in order to assess adequacy and convergence behavior. While every chemical system poses its own challenges, certain rules of thumb apply. For example, in a chemical reaction where a bond is formed/broken, all of the orbitals involved in the bond must be included in the active space, as well as antibonding orbitals that typically significantly contribute to correlating the bonding electrons. Similarly, when several electronic states are under consideration, all those molecular orbitals involved in electronic excitations that connect the states must be included in the active space. More detailed considerations on the construction of multiconfigurational (MC)SCF wave functions in general[10] and for the special case of transition-metal compounds[17,18] may be found in the literature. Practical issues associated with memory and disk storage limit the size of the active space in modern software packages to about 15 electrons in 15 orbitals, which is on the order of $1 \times 10^6$ to about $16 \times 10^6$ CSFs depending on spin and spatial symmetry. This restriction on active space size is the most severe limitation of the CASSCF (and subsequent CASPT2) model and renders it inapplicable to systems where a larger active space is chemically necessary.

When the active space *has* been adequately chosen, the CASSCF wave function will include the most important CSFs in the full CI wave function. In particular, it includes all near-degenerate configurations, which describe static, *nondynamical*, correlation effects, as found, for example, in bond-breaking processes. The CASSCF wave function can thus qualitatively exhibit correct behavior over an entire chemical process, e.g., mapping the potential energy surface for a chemical reaction or studying a multistate photochemical conversion. Nevertheless, computed CASSCF energies are typically not very accurate, as smaller active spaces fail to include those CSFs that are important for capturing remaining *dynamical* correlation effects. Thus, including nondynamical correlation is as important for quantitative accuracy in the multiconfigurational approach as it is in cases where the HF single-determinantal approximation is applicable.

How can dynamical electron correlation be included? One method that has been used with some success is MRCI, where the most important CSFs of the CAS wave function are used as a multiconfigurational reference in a CI expansion that includes additional CSFs generated by single, double, or higher excitations from occupied orbitals of the reference to virtual orbitals.[19] This method, however, quickly demands enormous computational resources for systems with many electrons and also fails to be size extensive, although this latter problem can be corrected for in an approximate fashion.[20]

In a single configuration approach, the preferred choices for including dynamical correlation derive from size-extensive many-body theory and include coupled cluster (CC) methods or, if the system is too large, less demanding approximations such as second-order perturbation theory. Møller–Plesset second-order perturbation theory (MP2) has long been used to estimate electron correlation for single-determinantal ground states, and is known to give reasonably accurate results for structural, energetic, and other properties of molecular ground states when a single-determinantal reference is appropriate. The idea of using second-order perturbation theory with a multiconfigurational wave function was first suggested soon after the introduction of the CASSCF method[21] and a full implementation was accomplished in the late 1980s.[22,23] The resulting CASPT2 model is computationally more efficient than MRCI and is now the most widely used method to compute dynamical electron correlation effects for multiconfigurational (CASSCF) wave functions.

The principle is simple: One computes the second-order energy with a CASSCF wave function as the zeroth-order

approximation. That said, there are some issues in the multiconfigurational case that do not arise for single-determinantal MP2. In particular, one needs to define a zeroth-order Hamiltonian for which the CASSCF wave function is an eigenfunction, just as in MP2 the single-determinantal HF wave function is an eigenfunction of the Hamiltonian defined as the sum of one-electron Fock operators. The multiconfigurational zeroth-order Hamiltonian should preferably also be a one-electron operator in order to avoid too complicated a formalism. We next address those technical features of CASPT2 that are relevant to the current implementation of RASPT2.

We seek an approximate Hamiltonian $\hat{H}^{(0)}$, such that the root function $\Psi^{(0)}$ is an unperturbed eigenfunction satisfying

$$\hat{H}^{(0)}\Psi^{(0)} = E_0\Psi^{(0)}, \qquad (1)$$

with eigenvalue $E_0$. The conventional single-reference Rayleigh–Schrödinger perturbation theory then gives for the first-order wave function

$$(\hat{H}^{(0)} - E_0)\Psi^{(1)} = -(\hat{H} - E_0)\Psi^{(0)}, \qquad (2)$$

$$\Psi^{(1)} = -(\hat{H}^{(0)} - E_0)^{-1}(\hat{H} - E_0)\Psi^{(0)}, \qquad (3)$$

where $\hat{H}$ is the full CI Hamiltonian, i.e., the exact Hamiltonian in the relevant Fock space restricted only by the use of a finite set of one-electron basis functions, and the inverse is taken in the space of functions normal to $\Psi^{(0)}$.

The most simple and convenient form for the operator $\hat{H}^{(0)}$ is a noninteracting Hamiltonian, which in second quantized form is associated with orbitals that diagonalize a one-electron Hamiltonian. With a single-determinantal root function, this defines Møller-Plesset perturbation theory. With a multiconfigurational root function, a simple one-electron $\hat{H}^{(0)}$ cannot be used, as a multiconfigurational $\Psi^{(0)}$ is generally not an eigenfunction of such a noninteracting Hamiltonian. In the CASPT2 model, this is addressed by the introduction of projection operators. Thus, $\hat{H}^{(0)}$ is defined as

$$\hat{H}^{(0)} = \hat{P}_{CAS}\hat{H}\hat{P}_{CAS} + \hat{P}_{SD}\hat{F}\hat{P}_{SD} + \hat{P}_{TQ}\hat{F}\hat{P}_{TQ} + \ldots , \qquad (4)$$

where $\hat{P}_{CAS}$ projects onto the root function, $\hat{P}_{SD}$ onto the space spanned by single and double replacement states, and $\hat{P}_{TQ}\ldots$ onto the spaces spanned by higher order excitations. This form ensures that the first-order wave function $\Psi^{(1)}$ can be found in the finite-dimensional space $S_{SD}$.

The generalized Fock matrix $\hat{F}$ is, as usual, of the form

$$\hat{F} = \sum_{pq} F_{pq}\hat{E}_{pq}, \qquad (5)$$

where $\hat{E}_{pq}$ is the conventional spin-summed excitation operator in second quantization, and $F_{pq}$ is the matrix element for molecular orbitals $\psi_p$, $\psi_q$ (we use the convention that orbital indices are denoted $i, j, k, l$ for inactive orbitals, $t, u, v, x$ for active ones, $a, b, c, d$ for virtual orbitals, and $p, q, r, s$ in the absence of any particular specification).

The molecular orbitals are to some extent arbitrary, in the sense that the root function is equally well described if any unitary transformation is applied that does not mix the inactive, active, and external orbitals of the CASSCF calculation. This introduces another difference compared to single-determinantal MP2: While the orbitals can be chosen to make the Fock matrix consist of diagonal submatrices with orbital energies on the diagonal, there may remain nonzero elements that couple inactive/active, inactive/external, or active/external orbitals. When using the CASPT2 subdivision of the spaces, as shown by Eq. (4), multiconfigurational cases can show size inextensivity, but this deficiency is usually small in magnitude.

A final distinction between single-determinantal and multideterminantal root functions $\Psi^{(0)}$ is that, in the former, the wave function expansion can either be regarded to be in terms of single determinants having one or more replacements of orbitals, or in terms of contributions generated by the action of excitation operators on the root function; in either case, these determinants are eigenfunctions of $\hat{H}^{(0)}$. For multideterminantal root functions, however, these two *Ansätze* are very different, in that the first can require extremely large expansions, while the second gives a dimension of the expansion space that is not much larger than that for a similar MP2 calculation. An advantage with the first approach is that the $\hat{H}^{(0)}$ operator can be defined to be diagonal in the expansion space. In CASPT2, however, we have chosen the latter *Ansatz*. The $\Psi^{(1)}$ wave function is then defined in terms of two-electron excitations from the root function,

$$\Psi^{(1)} = \sum_{pqrs} t_{pqrs}\hat{E}_{pqrs}\Psi^{(0)}. \qquad (6)$$

Equation (3) can then be satisfied by the solution of a system of linear equations in the variables $t_{pqrs}$ appearing in Eq. (6).

Not all possible excitations covered by Eq. (6) are necessary. If the CI expansion in the CASSCF root function is converged (not necessarily with optimized orbitals), terms with four active orbital indices are not needed. Of the remaining possibilities, only combinations with $p$, $r$ active or virtual and with $q$, $s$ active or inactive are needed. The excitations are then classified into eight types:

| Internal: | Semiinternal: | External: |
|---|---|---|
| $\hat{E}_{tiuv}$ | $\hat{E}_{atuv}$ | $\hat{E}_{atbu}$ |
| $\hat{E}_{tiuj}$ | $\hat{E}_{aitu}$ or $\hat{E}_{tiau}$ | $\hat{E}_{aibt}$ |
| | $\hat{E}_{tiaj}$ | $\hat{E}_{aibj}$ |

The resulting Fock matrix cannot in general be fully diagonalized. However, the part consisting of the inactive/inactive submatrix, the active/active submatrix, and the external/external submatrix can be diagonalized, while changing at the same time the CI expansion coefficients, such that the root function is unchanged while the above-mentioned block-diagonal parts are represented by orbital energies in the usual way:

$$\hat{F} = \sum_p \varepsilon_p \hat{E}_{pp} + \sum_{ti} F_{ti}(\hat{E}_{ti} + \hat{E}_{it}) + \sum_{ai} F_{ai}(\hat{E}_{ai} + \hat{E}_{ia})$$
$$+ \sum_{au} F_{au}(\hat{E}_{au} + \hat{E}_{ua}).$$

Parametrization using the coefficients $t_{pqrs}$ usually gives a very poorly conditioned equation system. This is addressed by defining new coefficients, according to

$$\Psi^{(1)} = \sum_{pqrs} c_\alpha \hat{X}_\alpha \Psi^{(0)}, \tag{7}$$

$$\hat{X}_\alpha = \sum_{pqrs} T_{pqrs,\alpha} \hat{E}_{pqrs}, \tag{8}$$

$$t_{pqrs} = \sum_\alpha T_{pqrs,\alpha} c_\alpha. \tag{9}$$

The transformation matrices have been determined such that the individual terms $\hat{X}_\alpha \Psi^{(0)}$ in the first-order wave function are orthonormal, and thus noninteracting for the block-diagonal parts of $\hat{H}^{(0)}$. The CASPT2 Eq. (3) then becomes a system of linear equations with coefficient matrix $\mathbf{A}$ and right-hand side (RHS) vector $\mathbf{v}$ whose elements are

$$A_{\alpha,\beta} = \langle \Psi^{(0)} | \hat{X}_\alpha^\dagger (\hat{H}^{(0)} - E_0) \hat{X}_\beta | \Psi^{(0)} \rangle,$$

$$v_\alpha = \langle \Psi^{(0)} | \hat{X}_\alpha^\dagger (\hat{H}^{(0)} - E_0) | \Psi^{(0)} \rangle.$$

The equation matrix is not handled in full component form but is represented by a number of factorized matrices and is strongly dominated by its diagonal, with couplings between submatrices iteratively handled by a preconditioned conjugate gradient solver. Upon convergence, usually after about 5–15 iterations, a solution for

$$\mathbf{As} = -\mathbf{v} \quad \text{i.e.,} \quad \sum_\beta A_{\alpha,\beta} s_\beta = -v_\alpha \tag{10}$$

is obtained, which provides a solution to the original CASPT2 Eq. (3) in the form

$$\Psi^{(1)} = \sum_\beta s_\beta \hat{X}_\beta | \Psi^{(0)} \rangle = \sum_{pqrs} \left( \sum_\beta T_{pqrs,\beta} s_\beta \right) \hat{E}_{pqrs} | \Psi^{(0)} \rangle. \tag{11}$$

Here $\mathbf{s}$ denotes the expansion coefficients of the first-order wave function in the orthonormal basis $\hat{X}_\alpha \Psi^{(0)}$. The equation system would be directly solved if the inactive-active, inactive-virtual, and active-virtual couplings were all zero. As these couplings are small, however, the direct solution of the diagonal part is a very efficient preconditioner of the full system.

## B. The RASSCF/RASPT2 method

An alternative to the CASSCF method exists that has seen comparatively little use, namely, the RASSCF method.[24,25] In this model, the active subspace is itself divided into three distinct regions: RAS1, RAS2, and RAS3 (see Fig. 1). The RAS2 region is identical to the active region in a CAS calculation, i.e., all possible spin- and symmetry-adapted CSFs that can be constructed from the orbitals in RAS2 are included in the multiconfigurational wave function. The RAS1 and RAS3 spaces, on the other hand, permit the generation of additional CSFs subject to the restriction that a maximum number of excitations may occur from RAS1, which otherwise contains only doubly occupied orbitals, and a maximum number of excitations may occur into RAS3, which otherwise contains only external orbitals.

Many different types of RAS wave functions can be constructed. For example, if one leaves RAS1 fully occupied and RAS3 empty, i.e., if the excitation maxima referred to above are both zero, then one identically obtains the CASSCF wave function for space RAS2. As another example, if the RAS2 space is defined to be empty, then the choice of excitation maxima delivers a RASSCF wave function that includes all single, double, etc., excitations within the RAS1/RAS3 window, i.e., a SDTQ, etc., CI wave function. The formalism is clearly quite flexible.

A key feature of the RASSCF wave function is that, provided the maximum number of RAS1/RAS3 excitations is relatively few, the number of CSFs associated with a given RAS protocol can be substantially smaller than for the CASSCF alternative defined over the same active space. The RASSCF model thus has the potential to permit multiconfigurational calculations with larger active spaces than can be employed with the CASSCF method. The challenge with a RASSCF wave function, however, is how to go about including the effects of dynamical electron correlation. In particular, second-order perturbation theory is not equally straightforward to apply in the case of a RASSCF wave function.

In order to address this issue, we have proceeded in the following manner, which represents in some sense the simplest approach (possible improvements are discussed below in Sec. IV). In the current RASPT2 model, the effective Fock matrix is expanded from the $3 \times 3$ block structure of the CASPT2 model to a $5 \times 5$ block structure where the new blocks are derive from separating the single CASPT2 active/active block into a $3 \times 3$ set of subblocks defined by the RAS1, RAS2, and RAS3 orbital spaces. This introduces a fundamental difference in the two PT2 implementations insofar as orbital rotations that couple different RAS spaces, i.e., RAS1 and RAS2, RAS1, and RAS3, and RAS2 and RAS3, are not allowed. Thus, the diagonalization of the active part of the Fock matrix is not complete in RASPT2, as it is in CASPT2, but instead nonzero elements may remain in the parts that couple different RAS spaces. Some additional technical points must be addressed in formulating and diagonalizing the RASPT2 Fock matrix, some of which arise because the first-order interacting space $S_{SD}$ is not as straightforwardly described in terms of orbital excitations but also depends on the occupation numbers of the CSFs.

We note that all except one of the CASPT2 excitation classes described above involve at least one active orbital. In the RASPT2 model, if an excitation creates an electron in a RAS3 orbital, or annihilates an electron in a RAS1 orbital, then a subset of the CSFs that are produced will fulfill the RAS restrictions, while the rest will not. However, in every case the excitation is combined with another excitation that either annihilates an electron in an inactive orbital or creates
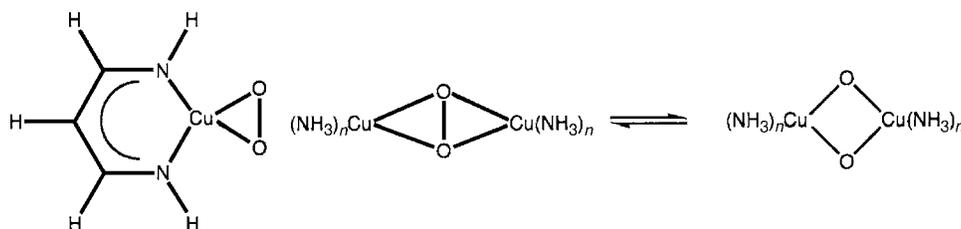
FIG. 2. Molecular structures for $(C_3N_2H_5)CuO_2$ and $\{[Cu(NH_3)_n]_2O_2\}^{2+}$ isomerism.

an electron in an external orbital, so all resulting CSFs will indeed belong to the first-order interacting space $S_{SD}$. Thus, as long as the remaining class of fully internal excitations is ignored, essentially the same formalism as in CASPT2 can be used, except that the active-active part of the Fock matrix is no longer fully diagonal. However, the matrix **A** as well as the RHS **v** of Eq. (10), or rather the data sets used to represent them in the actual calculations, involve reduced density matrices of only up to three particles (using active orbital indices only). These are computed using intermediate wave functions, which also must obey the RAS restrictions. By making use of conjugation and index permutation symmetries, all intermediate wave functions can be constrained to obey these restrictions.

## III. APPLICATION TO SUPPORTED CuO₂ AND Cu₂O₂ SYSTEMS

We now examine the performance of the RASPT2 model for two challenging problems associated with the activation of $O_2$ by copper. Because of favorable combinations of co-valency and oxidation/reduction potentials, the activation of molecular oxygen by its coordination to one or two supported (i.e., ligated) Cu(I) ions is common to a number of biological and inorganic catalytic processes.[26–39] In the case of monocopper species $LCuO_2$, where $L$ is a general ligand or ligands, one possible oxidation state that may be assigned to the complex is $LCu(II)O_2(-)$; thus, the copper atom has been oxidized by one electron and the $O_2$ fragment is formally a superoxide radical anion. Similarly, in the case of dicopper species $(LCu)_2O_2$, one possible oxidation state of the complex is formally $[LCu(II)]_2[(O_2)(2-)]$; in this instance, each copper atom has been oxidized by one electron and the $O_2$ fragment is formally a peroxide dianion. In both of these cases, the resulting compounds with a variety of ligands can have singlet ground states that exhibit substantial biradical character because of the spin separation associated either with two $d^9$ Cu(II) ions or one such ion and a super-oxide radical anion.[40–52] Wave function theories restricted to a single determinant are poorly suited to the description of such species since singlet biradicals are intrinsically two determinantal.[53,54] Moreover, even when oxidation states more likely to be characterized as closed shell in nature are considered, e.g., $[LCu(III)]_2[O(2-)]_2$, computational studies have found that large contributions from dynamical correlation effects influence relative isomer energetics.[40–42,47–49,51,52]

In this section, we apply the RASPT2 method to two problems previously studied in considerable detail using a wide range of theoretical models (see Fig. 2).

The first case considers the singlet-triplet splitting in $LCuO_2$, $L = 1,3$-diketiminate[44,52] while the second examines the relative energies of the isomeric peroxo- and bis-$\mu$-oxo forms of $\{[Cu(NH_3)_n]_2O_2\}^{2+}$ ($n = 0, 1, 2, 3$). In each case, our goal is primarily to compare the performance of different RASPT2 and CASPT2 protocols one to another, noting that in the latter case, i.e., the $\{[Cu(NH_3)_n]_2O_2\}^{2+}$ system, prior experience has indicated that it is impossible to choose a CAS sufficiently large to provide converged, balanced results for the CASPT2 energetics of the isomeric equilibrium.[49]

### A. Computational details

For $(C_3N_2H_5)CuO_2$, structures for the lowest singlet and triplet state were obtained using B3LYP-DFT (Refs. 55–58) [making use of the Stuttgart pseudopotential and associated basis functions for Cu (Refs. 59 and 60) and 6-31G(d) basis sets[61] for other atoms]. Both structures are planar and have $C_{2v}$ symmetry. They are positioned in the $xy$-plane, with the Cu–O₂ bonds bisected by the $x$-axis (i.e., the $C_2$ axis). All calculations on $\{[Cu(NH_3)_n]_2O_2\}^{2+}$ were performed on structures taken from Ref. 49. The molecules were positioned with the Cu₂O₂ core in the $xy$-plane, the two Cu atoms on the $x$-axis, and the two oxygen atoms on the $y$-axis. As such, in both types of molecules, the orbitals primarily involved in the Cu–O bonding are Cu $3d_{xy}$, O $2p_x$, and O $2p_y$.

Two different basis sets were used in these calculations. The smallest basis set, denoted as BS1, consists of the Stuttgart pseudopotential and associated basis functions for Cu,[59,60] combined with atomic natural orbital (ANO)-L basis sets for the other atoms,[62] contracted to $[4s3p2d]$ for O and N and $[2s1p]$ for H. The larger BS2 basis set is built from ANO-rcc basis sets[63,64] on all atoms, contracted to $[7s6p4d3f2g]$ for Cu, $[4s3p2d1f]$ for N and O (all such atoms are directly coordinated to copper), $[4s3p2d]$ for C [appearing only in $(C_3N_2H_5)CuO_2$, and not directly bound to copper], and $[3s1p]$ for H. For the calculations with BS2, scalar relativistic corrections were included using a (standard second-order) Douglas–Kroll–Hess Hamiltonian. All calculations on $(C_3N_2H_5)CuO_2$ were performed with BS2. For $\{[Cu(NH_3)_n]_2O_2\}^{2+}$, most calculations were performed with BS1. This basis set was also used in previous studies[49,50] on $\{[Cu(NH_3)_n]_2O_2\}^{2+}$. Since we are also using the structures reported there, the present RASPT2 results are directly comparable to the DFT and completely renormalized (CR) CC results (CR-CC) from that work. For $\{[Cu(NH_3)_2]_2O_2\}^{2+}$ and $\{[Cu(NH_3)_3]_2O_2\}^{2+}$, a number of RASPT2 results obtained with BS2 are also presented.

The largest RASSCF calculations performed included all

valence electrons originating from occupied Cu $3d$ and O $2p$ atomic orbitals in an active space consisting of all valence orbitals and a second correlating orbital for each of them (i.e., Cu $3d,4d$, and O $2p,3p$). For $\{[Cu(NH_3)_n]_2O_2\}^{2+}$, this involves 28 electrons in 32 orbitals. For $(C_3N_2H_5)CuO_2$, 18 valence electrons were correlated in 21 orbitals, i.e., all Cu $3d,4d$ and O $2p,3p$ orbitals were included, except for one O $3p$ orbital corresponding to the unoccupied $\sigma_y^*$ orbital of $O_2^{2-}$. Smaller active spaces were constructed as follows:

- For $(C_3N_2H_5)CuO_2$, by removing the O $3p$ orbitals, as well as the O $2p_z$ $\pi(b_2)$ orbital, which is not involved in the Cu–$O_2$ bonding and is doubly occupied in both considered states. The other O $2p_z$ orbital, $\pi^*(a_2)$, is depopulated in the $^3B_2$ state and should therefore be active in all calculations. This reduced (16 in 15) active space still includes the static correlation effects connected to the Cu–$O_2$ bond as well as the Cu $3d$ *double-shell* effect.[65,66] The latter effect is moved to the perturbation treatment by further reducing the active space to (8 in 6), now only containing the Cu $3d_{xy}$, O $2p_{x,y}$ combinations as well as the O $2p_z$ $\pi^*(a_2)$ orbital.

- For $\{[Cu(NH_3)_n]_2O_2\}^{2+}$, by removing first the O $2p_z,3p_z$ orbitals, giving rise to 24 electrons in 28 orbitals, and second by removing also the O $3p_{x,y}$ orbitals, resulting in a (24 in 24) active space, including important correlation effects related to the Cu–O bonds and the Cu $3d$ double-shell effect. Removing all Cu $4d$ as well as the doubly occupied Cu $3d$ orbitals further reduces this active space to a minimalist (8 in 6), i.e., the bonding and antibonding combinations of both Cu $3d_{xy}$ and the O $2p_{x,y}$ orbitals.

The calculations are denoted as RASPT2$(n_{ae}$ in $n_{ao})/(n_{ae2}$ in $n_{ao2})/n$, with $n=2–5$ indicating the maximum number of electrons excited from RAS1 or into RAS3, $(n_{ae}$ in $n_{ao})$ describing the global RAS(1–3) active space, and $(n_{ae2}$ in $n_{ao2})$ describing that part of the global active space assigned to RAS2, i.e., that part in which all possible symmetry-adapted excitations are considered. The RAS2 space was left empty in calculations on $\{[Cu(NH_3)_n]_2O_2\}^{2+}$, but for $(C_3N_2H_5)CuO_2$ we considered either an (8 in 6) RAS2 space, as described above, or we left RAS2 empty for the singlet state, and populated it with the two singly occupied orbitals for the $^3B_2$ state. Calculations without a RAS2 space are denoted as RASPT2$(n_{ae}$ in $n_{ao})//n$. Calculations on $(C_3N_2H_5)CuO_2$ with an (8 in 6) RAS2 space are only feasible for $n=2$, and for $n=3$ with the smaller global active spaces. Calculations with $n=4–5$, or with $n=3$ combined with the largest global active space, were only possible when performed with the state-specific empty/(2 in 2) RAS2 space.

RASPT2 calculations were performed with the standard IPEA shifted $\hat{H}^{(0)}$ operator[67] by using an imaginary denominator shift (IS) of 0.1 a.u. For $(C_3N_2H_5)CuO_2$, intruder states appeared in some of the calculations with $n=3$. In those cases, the IS was increased to 0.20–0.25, taking the lowest value that gave rise to stable results. Two different types of RASPT2 calculations were performed. In the first, all core

TABLE I. Relative energies (kcal mol$^{-1}$) of the $^3B_2$ and $^1A_1$ states in $(C_3N_2H_5)CuO_2$. $\Delta E_{ST}=E(^3B_2)-E(^1A_1)$.

| Active space | $\Delta E_{ST}$ |
|---|---|
| CASPT2(8 in 6) | 17.8 |
| CASPT2(16 in 15) | 6.3 |
| RASPT2(16 in 15)//2 | −2.3 |
| RASPT2(16 in 15)/(8 in 6)/2 | 7.4 |
| RASPT2(18 in 21)/(8 in 6)/2 | 15.5 |
| RASPT2(16 in 15)//3[a] | 3.3 |
| RASPT2(16 in 15)/(8 in 6)/3 | 9.0 |
| RASPT2(18 in 21)/(8 in 6)/3[b] | 11.5 |
| RASPT2(16 in 15)//4 | 7.7 |
| RASPT2(18 in 21)//4 | 11.2 |

[a]IS=0.20.
[b]IS=0.25.

orbitals, including also the semicore Cu $3s,3p$ orbitals, were kept frozen, whereas in the second the latter four orbitals were included in the correlation treatment.

For $\{[Cu(NH_3)_n]_2O_2\}^{2+}$, a series of test calculations with different active spaces, basis sets, and a different number of correlated electrons was performed for the relative energy between the bis($\mu$-oxo) and peroxo structures of $\{[Cu(NH_3)_2]_2O_2\}^{2+}$ and $\{[Cu(NH_3)_3]_2O_2\}^{2+}$. For all four $\{[Cu(NH_3)_n]_2O_2\}^{2+}$ species, RASPT2(24 in 28)//4 calculations were performed for all structures (taken from Ref. 49) along the reaction path connecting the bis($\mu$-oxo) and peroxo structures. These calculations were performed with BS1 and without Cu $3s,3p$ correlation, so that they could be compared to the CR-CC results from Ref. 49 (which also did not include these electrons).

## B. Singlet-triplet splitting in the $(C_3N_2H_5)CuO_2$ system

Table I shows the RASPT2 results obtained for the relative energy $\Delta E_{ST}$ between the $^3B_2$ and $^1A_1$ states in $(C_3N_2H_5)CuO_2$ with different active spaces (BS2, Cu $3s,3p$ included in RASPT2). The first two lines show the results obtained from CASPT2 calculations with an (8 in 6) and (16 in 15) active spaces. A difference of more than 10 kcal/mol is found between the CASPT2 results for $\Delta E_{ST}$ starting from a reference wave function which either does, (16 in 15), or does not, (8 in 6), include the Cu $3d$ double-shell effect. This clearly illustrates the importance of taking care of this type of correlation in the zeroth-order variational step.

With the (16 in 15) active space, two different types of RASPT2 calculations are presented, one in which the correlation effects on the Cu–O bonds are described by a full CI in the (8 in 6) RAS2 space, and a second in which these effects are, together with the Cu $3d$-$4d$ correlation, treated by up to double, triple, or quadruple RAS1→RAS3 excitations. It is clear from the data in Table I that up to quadruple excitations are mandatory to describe the correlation effects on the Cu–O bonds. The differences between the results obtained from RAS(16 in 15)//$n$ calculations with and without a (8 in 6) RAS2 space are a sizable 9.6 kcal/mol for $n=2$, and still 5.7 kcal/mol for $n=3$. On the other hand, the $\Delta E_{ST}$ value

TABLE II. Relative energies (kcal mol$^{-1}$) of the bis($\mu$-oxo) and peroxo structures of $\{[Cu(NH_3)_2]_2O_2\}^{2+}$ and $\{[Cu(NH_3)_3]_2O_2\}^{2+}$. $\Delta E_{bp} = E(\text{bis}(\mu\text{-oxo})) - E(\text{peroxo})$.

| Active space | $\{[Cu(NH_3)_2]_2O_2\}^{2+}$ | | $\{[Cu(NH_3)_3]_2O_2\}^{2+}$ | |
| --- | --- | --- | --- | --- |
| | No Cu3$s$,3$p$ Correlated | With Cu3$s$,3$p$ Correlated | No Cu3$s$,3$p$ Correlated | With Cu3$s$,3$p$ Correlated |
| | Calculations with BS1 | | | |
| CASPT(8 in 6) | 18.0 | −20.9 | −8.8 | −13.6 |
| RASPT2(24 in 24)//2 | −10.2 | −8.7 | −3.5 | −2.1 |
| RASPT2(24 in 24)/(8 in 6)/2 | −8.8 | −6.5 | 3.6 | 3.9 |
| RASPT2(24 in 28)/(8 in 6)/2 | −6.9 | −5.5 | 4.0 | 3.3 |
| RASPT2(28 in 32)/(8 in 6)/2 | −4.8 | −4.3 | 5.4 | 4.2 |
| RASPT2(24 in 24)//3 | −8.0 | −5.5 | 0.6 | 2.9 |
| RASPT2(24 in 24)/(8 in 6)/3 | −5.2 | −3.6 | 6.8 | 7.1 |
| RASPT2(24 in 24)//4 | −6.6 | −5.7 | 4.1 | 3.9 |
| RASPT2(24 in 28)//4 | −1.8 | −1.2 | 7.6 | 7.0 |
| RASPT2(28 in 32)//4 | −0.7 | −0.4 | 8.0 | |
| RASPT2(24 in 24)//5 | −6.6 | −4.1 | | |
| | Calculations with BS2 | | | |
| CASPT2(8 in 6) | | −26.2 | | −20.6 |
| RASPT2(24 in 24)//4 | | −4.5 | | −1.0 |
| RASPT2(24 in 28)//4 | | −2.6 | | 1.8 |
| RASPT2(28 in 32)//4 | | −3.3 | | |

obtained with RAS(16 in 15)//4, 7.7 kcal/mol, is quite close the more complete CASPT2(16 in 15) result, 6.3 kcal/mol, indicating that the important nondynamical correlation effects in this system, both on the bonding interactions and the Cu 3$d$ double-shell effect, may be captured by a (MC)SCF calculation including only up to quadruple excitations. Furthermore, the difference in $\Delta E_{ST}$ between RASPT2(16 in 15)/(8 in 6)/2 and CASPT2(16 in 15) is moderate, 1.1 kcal/mol. This suggests that for this monocopper system the 3$d$ double-shell effect may already quite accurately be described by a RASSCF wave function including only up to double 3$d \rightarrow 4d$ excitations.

By increasing the size of the active space from (16 in 15) to (18 in 21) oxygen 2$p$-3$p$ correlation is introduced in the zeroth-order wave function. The effect is significant: 2.5–3.5 kcal/mol even with $n=3$ or 4. The final results obtained from either RAS(18 in 21)//4 or RAS(18 in 21)/(8 in 6)/3 are similar, 11.2–11.5 kcal/mol, suggesting that this value is approaching convergence, and represents our best estimate for the correct value for these geometries. On the other hand, including only up to double RAS1/RAS3 excitations obviously fails to suffice for an accurate description of the O 2$p$-3$p$ correlation effects, leading to a result (15.5 kcal/mol) which is too high by about 4 kcal/mol.

## C. Relative energy of peroxo- and bis-$\mu$-oxo isomers of $\{[Cu(NH_3)_n]_2O_2\}^{2+}$ ($n=0,1,2,3$)

Table II shows the RASPT2 results obtained for the relative energy $\Delta E_{bp}$ between the bis($\mu$-oxo) and peroxo structures of $\{[Cu(NH_3)_2]_2O_2\}^{2+}$ and $\{[Cu(NH_3)_3]_2O_2\}^{2+}$ with dif-

ferent active spaces, numbers of correlated electrons, and basis sets. Best estimates for this quantity based on prior many-body and DFT calculations for equivalent structures and basis sets[49] are about −2 kcal/mol for $n=2$ and 8 kcal/mol for $n=3$.

Once again, correlation effects on bonding in the Cu$_2$O$_2$ core may be described by an (8 in 6) active space, but in this case including the description of the Cu 3$d$ double-shell effect in the reference wave function requires a (24 in 24) active space, which is far too large for a CASSCF treatment. The lack of Cu 3$d$-4$d$ correlation in the zeroth-order wave function is the main reason for the failure of the CASPT2 treatment in the original[41] and later[47,49,68] CASPT2 studies on this subject. All these studies were performed with moderately sized basis sets (comparable to BS1) and with active spaces starting from the (8 in 6) space used here, possibly extended with other valence (O 2$s$, O 2p$_z$) or virtual (O 3$p$) orbitals. However, limitations on the size of the CAS space prevented the inclusion of the full set of Cu 3$d$, 4$d$ orbitals, and this invariably led to erroneous CASPT2 results, grossly overestimating (more than 20 kcal/mol) the stability of the bis($\mu$-oxo) isomer relative to the peroxo isomer. As the results in Table II indicate, including the Cu 3$d$ double-shell effect in the (24 in 24) active space leads to a relative stabilization of the peroxo structure by up to 14 kcal/mol for $\{[Cu(NH_3)_2]_2O_2\}^{2+}$ and up to 20 kcal/mol for $\{[Cu(NH_3)_3]_2O_2\}^{2+}$ (for the BS1 calculations).

As proved true for $(C_3N_2H_5)CuO_2$, properly accounting for correlation effects on the Cu–O bonding requires inclusion in the reference wave function of excitations at least up

TABLE III. Relative energies (kcal mol$^{-1}$) of the bis($\mu$-oxo) and peroxo structures. RASPT2(24 in 28)//4 calculations without Cu$3s$, $3p$ correlated, compared to best estimates in parentheses, performed with BS1. [Best estimates are rounded to nearest unit. For the first two molecules they are CR-CC results, for the last two molecules they are an average of CR-CC results, and (similar) DFT results from the three non-hybrid density functionals. Full details of prior theoretical models are available in Ref. 49.]

| Molecule | $F$ | | | | | |
|---|---|---|---|---|---|---|
| | 0% | 20% | 40% | 60% | 80% | 100% |
| $[Cu_2O_2]^{2+}$ | 28.6 | 21.2 | 15.1 | 7.1 | 0.8 | 0.0 |
| | (34) | (24) | (16) | (8) | (2) | (0) |
| $\{[Cu(NH_3)]_2O_2\}^{2+}$ | 25.2 | 16.6 | 9.4 | 1.9 | −3.5 | 0.0 |
| | (30) | (20) | (12) | (3) | (−2) | (0) |
| $\{[Cu(NH_3)_2]_2O_2\}^{2+}$ | −1.8 | −1.6 | 0.8 | −0.8 | −4.7 | 0.0 |
| | (−3) | (−1) | (2) | (2) | (−2) | (0) |
| $\{[Cu(NH_3)_2]_2O_3\}^{2+}$ | 7.6 | 7.2 | 9.2 | 6.3 | 0.3 | 0.0 |
| | (8) | (9) | (12) | (10) | (4) | (0) |

to quadruples between the orbitals involved: the $\Delta E_{bp}$ values obtained from RASPT2(24 in 24)/(8 in 6)/$n$ are systematically larger than those from corresponding RASPT2(24 in 24)//$n$ calculations, by 2–3 kcal/mol for $\{[Cu(NH_3)_2]_2O_2\}^{2+}$ and by 5–7 kcal/mol for $\{[Cu(NH_3)_3]_2O_2\}^{2+}$. However, as compared to $(C_3N_2H_5)CuO_2$, a more significant increase (3 kcal/mol) of $\Delta E_{bp}$ is in this case obtained by addressing the Cu $3d$ double-shell effect by up to triple rather than up to double RAS1→RAS3 excitations. Of course, this increase is *a priori* to be expected for size-extensivity reasons, since we are now dealing with two instead of only one copper center. Furthermore, it should be noted that the $\Delta E_{bp}$ values obtained from RASPT2(24 in 24)//4 are systematically lower than those obtained from RASPT2(24 in 24)/(8 in 6)/3 or from RASPT2(24 in 24)//5 when Cu semicore orbitals are included (see below). This suggests that with RASPT2(24 in 24)//4 the description of correlation effects on the Cu–O bonds may not yet be fully converged with respect to the excitation level in the active space, and that RASPT2(24 in 24)/(8 in 6)/4 would give $\Delta E_{bp}$ values that are higher by 3–5 kcal/mol. Unfortunately, such a calculation exceeds the practical limits of our current RASPT2 implementation. However, even with a remaining uncertainty of this magnitude, it is clear that the results obtained from the present (24 in 24) RASPT2 protocol represent a considerable improvement over all previous CASPT2 calculations.

A further significant (3–5 kcal/mol) increase of the $\Delta E_{bp}$ values is obtained by extending the active space from RAS(24 in 24)//4 to RAS(24 in 28)//4 by including correlating O $3p$ orbitals for the O $2p_{x,y}$ orbitals involved in the Cu–O bonds. Including also the O $2p_z, 3p_z$ couples (28 in 32) has a minor effect: 1 kcal/mol or less with BS1 and becoming slightly negative with BS2. As such, we believe that the present calculations are converged with respect to the size of the total active space.

Finally, we consider the effect of Cu $3s,3p$ semicore correlation (columns 2 and 4 of data in Table II) and basis set effects. Starting from the CASPT2(8 in 6) active space, add-

ing the Cu $3s,3p$ electrons to the correlation treatment has a significant effect on the relative energies of the two structures, stabilizing the bis($\mu$-oxo) structure by 3 kcal/mol for $\{[Cu(NH_3)_2]_2O_2\}^{2+}$, and by 5 kcal/mol for $\{[Cu(NH_3)_3]_2O_2\}^{2+}$. However, the effect is reduced in the RASPT2 results obtained with larger active spaces, and in some of these calculations even reverses its sign. This seems to indicate that transition-metal semicore correlation effects may, in fact, be overestimated by CASPT2 based on a too small active space. A similar phenomenon, although less pronounced, is observed when comparing the results obtained with different basis sets. Increasing the basis sets to BS2 significantly stabilizes the bis($\mu$-oxo) structure with respect to the peroxo structure for both $\{[Cu(NH_3)_2]_2O_2\}^{2+}$ and $\{[Cu(NH_3)_3]_2O_2\}^{2+}$. However, the effect is again largest for the CASPT2(8 in 6) calculations and is reduced when performing RASPT2 with larger active spaces. Still, we note that for $\{[Cu(NH_3)_3]_2O_2\}^{2+}$ the "best" result for $\Delta E_{bp}$, obtained from RASPT2(24 in 28)//4, is reduced from 7.0 kcal/mol with BS1 to 1.8 kcal/mol with BS2, the latter number suggesting that both structures of this molecule are nearly degenerate in energy.

Prior studies of the bis($\mu$-oxo)/peroxo equilibrium have focused not only upon the relative energies of the two stationary points shown in Fig. 2, but also on the reaction coordinate generated by a linear transformation of one structure into the other. Table III shows the relative energies predicted from RASPT2(24 in 28)//4 calculations for the different structures along this reaction coordinate where $F$ indicates the percentage transformation from extreme $F=0$ (bis($\mu$-oxo)) to extreme $F=100$ (peroxo).

In Fig. 3, the RASPT2(24 in 28)//4 results for the particular case of $\{[Cu(NH_3)_3]_2O_2\}^{2+}$ are graphically compared to DFT and CR-CC results from one previous study[49] and MRCI results from another.[47] The RASPT2 reaction coordinate is, in general, in fair to good agreement with coordinates predicted from CR-CC, MRCI, and the non-hybrid BLYP density functional. While $\{[Cu(NH_3)_3]_2O_2\}^{2+}$ is a model system for which experimental results are not available, the
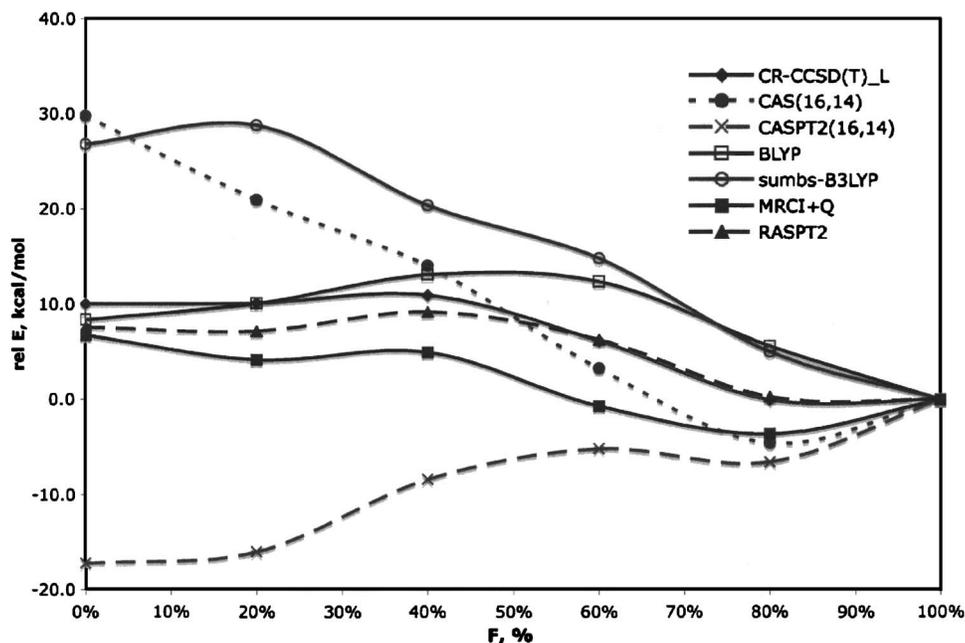
FIG. 3. Relative energy (kcal mol$^{-1}$) predicted from various levels of theory for a reaction coordinate linearly connecting the $\{[\text{Cu}(\text{NH}_3)_3]_2\text{O}_2\}^{2+}$ bis($\mu$-oxo) ($F=0\%$) and peroxo ($F=100\%$) structures shown in Fig. 2. The inset legend identifies the various theoretical models, which are discussed in more details in the text and, completely, in Ref. 49.

good agreement between CR-CC, MRCI, and non-hybrid density functional predictions has been interpreted to suggest that these levels of theory are indeed accurate for this isomerization. Moreover, non-hybrid DFT functionals such as BLYP have been shown to be quantitatively accurate for bis($\mu$-oxo)/peroxo equilibria that *have* been experimentally characterized;[51,69] such cases involve support of the copper atoms by larger, synthetically convenient bi- and tridentate ligands. Thus, to aid in interpretation of Table III, we report best estimate values for the isomerization coordinates of $[\text{Cu}_2\text{O}_2]^{2+}$, $\{[\text{Cu}(\text{NH}_3)]_2\text{O}_2\}^{2+}$, $\{[\text{Cu}(\text{NH}_3)_2]_2\text{O}_2\}^{2+}$, and $\{[\text{Cu}(\text{NH}_3)_3]_2\text{O}_2\}^{2+}$ that are taken from CR-CC calculations in the first two instances and an average of CR-CC and non-hybrid DFT calculations in the latter two instances.[49] With respect to the RASPT2(24 in 28)//4 model, there is still a small systematic tendency to overestimate the stability of the bis($\mu$-oxo) isomer relative to the peroxo, but the situation is vastly improved compared to CASPT2 (see Fig. 3), where the largest practical active space is (16 in 14).[49] We note that hybrid density functionals such as B3LYP also show substantial errors in their predictions for this isomerization, even after correcting for spin contamination using a broken-symmetry formalism (referred to as sum-bs in the inset legend of Fig. 3),[49] but the error is in the opposite direction to that of CASPT2.

## IV. DISCUSSION AND CONCLUSIONS

Some dynamical correlation effects are not addressed within the current RASPT2 *Ansatz*. When the RAS restrictions are used in order to allow large active spaces, the RAS1 and RAS3 subspaces should only handle dynamical correlation, and RAS2 should account for all nondynamical correlation. However, the subdivision into dynamical and nondynamical correlation is not well defined, and in addition the limited number of excitations allowed in the RAS1 and RAS3 subspaces can give significant size-extensivity errors. The situation would be much improved by extending the

model to include perturbative treatment of the fully internal excitations, i.e., excitations $\hat{E}_{tuvx}$-$\hat{E}_{utxv}$ from the RASSCF wave function. While such an improvement remains under consideration, implementation of these additional excitations is complicated because, while the RHS $\mathbf{v}$ of the RASPT2 equations still requires only the use of three-body density matrices, $\hat{H}^{(0)}$ would require fourth-order density matrices in the present formulation, and this is not practical with larger active spaces. Thus, the construction of this part of $\hat{H}^{(0)}$ will need new approximations in order to be efficiently implemented.

In addition, the structure of the doubly internal subblock is different from those associated with other excitation classes, since a subset of the CSF's that are involved have already been used in the RASSCF wave function. It will likely prove important to distinguish between those excited CSFs that continue to fulfill the RAS restrictions and those that do not, as is presently done for the excitation classes that are not fully internal. In our view, regarding the calculation as strictly a single-reference calculation with an internally contracted root function, it will likely prove simpler to use anti-Hermitian excitations of the form $\hat{E}_{tuvx}$-$\hat{E}_{utxv}$ and thus automatically produce linear combinations that are orthonormal to $\Psi^{(0)}$, rather than to use, e.g., additional projectors to separate out the interacting space. There will, of course, still be the additional problem of defining a suitable unperturbed Hamiltonian for the new excitations. However, even in the absence of this more complete implementation, the current RASPT2 model has proven valuable in the study of systems, such as the supported copper complexes above, where a large active space is required but relatively few orbitals need to be assigned to the fully flexible RAS2 subspace. Using the RAS1 and RAS3 spaces in analogy to the occupied and external spaces, respectively, and generating truncated CI wave functions at levels SD, SDT, or SDTQ, combines well with the subsequent perturbation theory accounting for additional

electron correlation, and we anticipate that this model will prove useful in many cases where CASPT2 is not currently practical.

## ACKNOWLEDGMENTS

[1] L. Gagliardi and B. O. Roos, Nature (London) **433**, 848 (2005).
[2] L. Gagliardi, M. C. Heaven, J. W. Krogh, and B. O. Roos, J. Am. Chem. Soc. **127**, 86 (2005).
[3] L. Gagliardi, P. Pyykkö, and B. O. Roos, Phys. Chem. Chem. Phys. **7**, 2415 (2005).
[4] D. Hagberg, G. Karlström, B. O. Roos, and L. Gagliardi, J. Am. Chem. Soc. **127**, 14250 (2005).
[5] L. Gagliardi, Theor. Chim. Acta **116**, 307 (2006).
[6] G. La Macchia, M. Brynda, and L. Gagliardi, Angew. Chem., Int. Ed. **45**, 6210 (2006).
[7] B. O. Roos and L. Gagliardi, Inorg. Chem. **45**, 803 (2006).
[8] P. Celani, H. Stoll, H. J. Werner, and P. J. Knowles, Mol. Phys. **102**, 2369 (2004).
[9] K. Dyall, J. Chem. Phys. **102**, 4909 (1995).
[10] M. W. Schmidt and M. S. Gordon, Annu. Rev. Phys. Chem. **49**, 233 (1998).
[11] H. A. Witek, H. Nakano, and K. Hirao, J. Chem. Phys. **118**, 8197 (2003).
[12] C. Angeli, M. Pastore, and R. Cimiraglia, Theor. Chim. Acta **117**, 743 (2007).
[13] B. O. Roos, in *Radiation Induced Molecular Phenomena in Nucleic Acids*, edited by M. K. Shukla and J. Leszczynski (Springer, Amsterdam, The Netherlands, 2008), pp. 125–156.
[14] L. Gagliardi and B. O. Roos, Chem. Soc. Rev. **36**, 893 (2007).
[15] B. O. Roos, P. R. Taylor, and P. E. M. Siegbahn, Chem. Phys. **48**, 157 (1980).
[16] B. O. Roos, in *Advances in Chemical Physics: Ab Initio Methods in Quantum Chemistry-II*, edited by K. P. Lawley (Wiley, Chichester, England, 1987), Chap. 69, p. 399.
[17] K. Pierloot, in *Nondynamic Correlation Effects in Transition Metal Coordination Compounds*, edited by T. R. Cundari (Dekker, New York, 2000), Chap. 5, pp. 123–158.
[18] K. Pierloot, Mol. Phys. **101**, 2083 (2003).
[19] P. E. M. Siegbahn, A. Heiberg, B. O. Roos, and B. Levy, Phys. Scr. **21**, 323 (1980).
[20] I. Hubač, P. Mach, and S. Wilson, Int. J. Quantum Chem. **89**, 198 (2002).
[21] B. O. Roos, P. Linse, P. E. M. Siegbahn, and M. R. A. Blomberg, Chem. Phys. **66**, 197 (1982).
[22] K. Andersson, P.-Å. Malmqvist, B. O. Roos, A. J. Sadlej, and K. Wolinski, J. Phys. Chem. **94**, 5483 (1990).
[23] K. Andersson, P.-Å. Malmqvist, and B. O. Roos, J. Chem. Phys. **96**, 1218 (1992).
[24] J. Olsen, B. O. Roos, P. Jørgensen, and H. J. A. Jensen, J. Chem. Phys. **89**, 2185 (1988).
[25] P.-Å. Malmqvist, A. Rendell, and B. O. Roos, J. Phys. Chem. **94**, 5477 (1990).
[26] K. D. Karlin and Y. Gultneh, Prog. Inorg. Chem. **35**, 219 (1987).
[27] E. I. Solomon and M. D. Lowery, Science **259**, 1575 (1993).
[28] K. D. Karlin and Z. Tyeklar, Adv. Inorg. Biochem. **9**, 123 (1994).
[29] P. L. Holland and W. B. Tolman, Coord. Chem. Rev. **192**, 855 (1999).
[30] N. Duran and E. Esposito, Appl. Catal., B **28**, 83 (2000).
[31] L. Que and W. Tolman, Angew. Chem., Int. Ed. **41**, 1114 (2002).
[32] C. Limberg, Angew. Chem., Int. Ed. **42**, 5932 (2003).
[33] L. M. Mirica, X. Ottenwaelder, and T. D. P. Stack, Angew. Chem., Int. Ed. **104**, 1013 (2004).
[34] E. A. Lewis and W. B. Tolman, Chem. Rev. **104**, 1047 (2004).
[35] T. Punniyamurthy, S. Velusamy, and J. Iqbal, Chem. Rev. **105**, 2329 (2005).
[36] S. Itoh, Curr. Opin. Chem. Biol. **10**, 115 (2006).
[37] J. P. Klinman, J. Biol. Chem. **281**, 3013 (2006).
[38] J. M. Bollinger, Curr. Opin. Chem. Biol. **11**, 151 (2007).
[39] C. J. Cramer and W. B. Tolman, Acc. Chem. Res. **40**, 601 (2007).
[40] C. J. Cramer, B. A. Smith, and W. B. Tolman, J. Am. Chem. Soc. **118**, 11283 (1996).
[41] M. Flock and K. Pierloot, J. Phys. Chem. A **103**, 95 (1999).
[42] C. J. Cramer, W. B. Tolman, K. H. Theopold, and A. L. Rheingold, Proc. Natl. Acad. Sci. U.S.A. **100**, 3635 (2003).
[43] P. E. M. Siegbahn, J. Biol. Inorg. Chem. **8**, 577 (2003).
[44] B. F. Gherman and C. J. Cramer, Inorg. Chem. **43**, 7281 (2004).
[45] N. W. Aboelella, S. Kryatov, B. F. Gherman, W. W. Brennessel, V. G. J. Young, Jr., R. Sarangi, E. Rybak-Akimova, K. O. Hodgson, B. Hedman, E. I. Solomon, C. J. Cramer, and W. B. Tolman, J. Am. Chem. Soc. **126**, 16896 (2004).
[46] C. R. Kinsinger, B. F. Gherman, L. Gagliardi, and C. J. Cramer, J. Biol. Inorg. Chem. **10**, 778 (2005).
[47] M. F. Rode and H. Werner, Theor. Chim. Acta **114**, 309 (2005).
[48] B. F. Gherman, D. E. Heppner, W. B. Tolman, and C. J. Cramer, J. Biol. Inorg. Chem. **11**, 197 (2006).
[49] C. J. Cramer, M. Wloch, P. Piecuch, C. Puzzarini, and L. Gagliardi, J. Phys. Chem. A **110**, 1991 (2006).
[50] C. J. Cramer, A. Kinal, M. Wloch, P. Piecuch, and L. Gagliardi, J. Phys. Chem. A **110**, 11557 (2006).
[51] B. F. Gherman and C. J. CramerCoord. Chem. Rev. (in press).
[52] C. J. Cramer, J. R. Gour, A. Kinal, M. Wloch, P. Piecuch, A. R. Moughal Shahi, and L. Gagliardi, J. Phys. Chem. A **112**, 3754 (2008).
[53] V. Bonacic-Koutecky, J. Koutecky, and J. Michl, Angew. Chem., Int. Ed. **26**, 170 (1987).
[54] C. J. Cramer, *Essentials of Computational Chemistry: Theories and Models*, 2nd ed. (Wiley, Chichester, 2004).
[55] A. D. Becke, Phys. Rev. A **38**, 3098 (1988).
[56] C. Lee, W. Yang, and R. G. Parr, Phys. Rev. B **37**, 785 (1988).
[57] A. D. Becke, J. Chem. Phys. **98**, 5648 (1993).
[58] P. J. Stephens, F. J. Devlin, C. F. Chabalowski, and K. J. Frisch, J. Phys. Chem. **98**, 11623 (1994).
[59] Institut für Theoretische Chemie, Universität Stuttgart, http://www.theochem.uni-stuttgart.de/
[60] D. Andrae, U. Häussermann, M. Dolg, H. Stoll, and H. Preuss, Theor. Chim. Acta **77**, 123 (1990).
[61] W. J. Hehre, L. Radom, P. v. R. Schleyer, and J. A. Pople, *Molecular Orbital Theory* (Wiley, New York, 1986).
[62] P.-O. Widmark, P.-Å. Malmqvist, and B. O. Roos, Theor. Chim. Acta **77**, 291 (1990).
[63] B. O. Roos, R. Lindh, P.-Å. Malmqvist, V. Veryazov, and P.-O. Widmark, J. Phys. Chem. A **109**, 2851 (2005).
[64] B. O. Roos, R. Lindh, P.-Å. Malmqvist, V. Veryazov, and P.-O. Widmark, J. Phys. Chem. A **109**, 6575 (2005).
[65] K. Andersson and B. O. Roos, Chem. Phys. Lett. **191**, 507 (1992).
[66] M. Merchán, R. Pou-Amérigo, and B. O. Roos, Chem. Phys. Lett. **252**, 405 (1996).
[67] G. Ghigo, B. O. Roos, and P.-Å. Malmqvist, Chem. Phys. Lett. **396**, 142 (2004).
[68] K. H. Marti, I. M. Ondik, G. Moritz, and M. Reiher, J. Chem. Phys. **128**, 014104 (2008).
[69] J. L. Lewin, D. E. Heppner, and C. J. Cramer, J. Biol. Inorg. Chem. **12**, 1221 (2007).